http://doi.org/10.29227/IM-2021-02-17 Received: 21 Jun 2021, Accepted: 19 Sep 2021, Published: 10 Nov 2021

Phase Diagrams of the Excitonic Insulator State: Analyzing the Excitonic Susceptibility

DO Thi Hong Hai[1], NGUYEN Thi Hau[1, *]

[1] Hanoi University of Mining and Geology, 18 Vien street, Hanoi, Vietnam

Corresponding author: nguyenthihau@humg.edu.vn

Abstract. In this paper, the formation of the excitonic insulator state in the rare-earth chalcogenides has been investigated through the extended Falicov-Kimball model. Adapting the unrestricted Hartree-Fock approximation, we have derived a set of explicitly self-consistent equations determining expectation values and the excitonic susceptibility in the system. Analyzing the excitonic susceptibility, we have established phase diagrams of the excitonic insulator state depending on the model parameters. The phase structures confirmed the excitonic insulator state is found at low temperature and between two critical values of the Coulomb interaction. The effect of the external pressure on the formation of the excitonic insulator state is also shown.

Keywords: Unrestricted Hartree-Fock approximation, Falicov-Kimball model, Excitonic insulator, Excitonic susceptibility, Rare-earth chalcogenide

1. Introduction

Excitonic insulator (EI) state has been predicted to occur in semimetal (SM) and semiconductor (SC) materials as the quantum condensation of electron-hole pairs. Although the first theoretical was proposed over a half-century ago [1-3], the nature of this state still has many things yet clarity as well as the ability to observe the experiment remains challenging. Because of the Coulomb attraction between electrons and holes, excitons can be established and if the temperature is low enough with a sufficiently high density, these excitons can condense forming a new spontaneous macroscopic phase-coherent quantum Bose-Einstein condensation (BEC) state [4], the so-called the excitonic insulator state.

In recent years, investigating some mixed-valent rare-earth chalcogenides and transition metal dichalcogenides has strongly supported the theoretical prediction and renewed the interest in the EI state. For instance, electrical and thermal transport properties in the pressure-sensitive mixed-valence rare-earth chalcogenide $TmSe_{0.45}Te_{0.55}$ have indicated a stabilized EI state at a temperature below 20 K [5-7]. Most recently, by using the momentum resolved electron energyloss spectroscopy, Kogar and coworkers have shown evidence for the excitonic condensation in the transition metal dichalcogenide semimetal 1T-$TiSe_2$ [8]. Besides, experimental results of the optical conductivity also have confirmed the existence of the EI state in narrow-gap semiconductor system Ta_2NiSe_5 [9, 10].

As an ordered state, the EI state might be distorted by the thermal fluctuations. Studying the influence of temperature on the EI state, therefore, is helpful. Phase diagrams depending on the temperature of the EI state have been experimentally reported [5, 6]. These phase diagrams show that the EI state occurs at low temperature with intermediate pressure around the semimetal-semiconductor transition. The phase diagrams of the EI state have also been addressed theoretically in a framework of the extended Falicov-Kimball model (EFKM) which covers direct *c*- and *f*-band hopping and admits the pairing of *c*-electrons with *f*-holes via the Coulomb interaction [11, 12]. In the SM regime with small Coulomb interaction, excitons might condense like Cooper pairs in the Bardeen-Cooper-Schrieffer (BCS) theory. On the other hand, in the SC regime, strong Coulomb interaction might formulate tight-binding excitons which then possibly condense like neutral atoms as in the theory of Bose-Einstein. A smooth BCS-BEC crossover of the EI state in the model is then discussed.

However, in the above studies, the description of the EI phase transition is only based on investigating the properties of the condensate order parameter. Moreover, recent studies of optical conductivity give us different views than the initial assumptions about the condensation formation of excitons. For example, in Ta_2NiSe_5 material, the optical conductivity calculated results from the density functional theory based electronic structure calculation and density-matrix renormalization group calculation or electronic states study in real space of low temperature phase release that excitons can be formed before the condensation happens even when the system is in the SM side [13, 14]. This is completely unconventional because one

always believes that this signature happens only in the SC phase, in the SM side the formation of excitons and their condensation state occur simultaneously [15]. Considering the excitonic susceptibility to clearly describe the condensation mechanism of the exciton systems is therefore necessary.

Rare-earth metals and their compounds are mainly used in industry and defense. They are also increasingly used in devices serving modern life such as: computer memory, Digital Video Disc, rechargeable battery, mobile phone, etc. In mixed-valence rare-earth chalcogenides, an exciton binding state of the 4*f* holes with the 5*d* electrons can be formed. At sufficiently low temperature, those excitons condense into the EI state. The effective mass of excitons is so small that they can condense at much higher temperatures than BEC critical temperature of atoms. Therefore, these material systems are being studied extensively in both science and technology [16]. In the present work, the EI state in rare-earth chalcogenides is discussed in the framework of the spinless EFKM, in which the hopping of the *f* electrons is involved. Using the unrestricted Hartree-Fock approximation, we obtain a set of self-consistent equations which allows us to determine the excitonic susceptibility function. From signatures of the static excitonic susceptibility function, we discuss in detail the phase structures of the EI state due to Coulomb attraction at low temperature.

This paper is organized as follows. In section 2, we introduce the theoretical approach of the present work. Here we present the 2D extended Falicov-Kimball model. and the unrestricted Hartree-Fock approximation developed for this model. In section 3, we outline numerical results where the phase diagrams of the EI state in the system are addressed. The conclusion is given in section 4.

2. Theoretical approach

In order to consider the electron-hole system in rare-earth chalcogenides, we use the EFKM with the Hamiltonian

$$\mathcal{H} = \mathcal{H}_0 + \mathcal{H}_{int} \tag{1}$$

with the non-interacting part of the electron system is given

$$\mathcal{H}_0 = \sum_{\mathbf{k}} \varepsilon_{\mathbf{k}}^c c_{\mathbf{k}}^\dagger c_{\mathbf{k}} + \sum_{\mathbf{k}} \varepsilon_{\mathbf{k}}^f f_{\mathbf{k}}^\dagger f_{\mathbf{k}} \tag{2}$$

where $c_{\mathbf{k}}^\dagger(c_{\mathbf{k}})$ and $f_{\mathbf{k}}^\dagger(f_{\mathbf{k}})$ are the creation (annihilation) operators of *c* and *f* electrons carrying momentum **k**, respectively. The electronic excitation energies in the tight-binding approximation are given by

$$\varepsilon_{\mathbf{k}}^{c(f)} = \varepsilon^{c(f)} - t^{c(f)}\gamma_{\mathbf{k}} - \mu \tag{3}$$

with $\varepsilon^{c(f)}$ are the on-site energies, $t^{c(f)}$ are the nearest-neighbor particle transfer amplitudes, and μ denotes the chemical potential. In two-dimensional hypercubic lattice, the nearest-neighbor hopping $\gamma_{\mathbf{k}}$ reads $\gamma_{\mathbf{k}} = 2(cosk_x + cosk_y)$.

The interacting part of the Hamiltonian $\mathcal{H}_{int}$ reads

$$\mathcal{H}_{int} = \frac{U}{N} \sum_{\mathbf{k},\mathbf{k}',\mathbf{q}} c_{\mathbf{k}+\mathbf{q}}^\dagger c_{\mathbf{k}'} f_{\mathbf{k}'-\mathbf{q}}^\dagger f_{\mathbf{k}} \tag{4}$$

here *U* is the Coulomb interaction between conduction *c* electrons and valence *f* electrons and *N* counts the number of lattice sites. In general, *c* – *c* and *f* – *f* Coulomb interactions might have been taken into account in the interaction part of the Hamiltonian in Eq. (4). However, the additional interactions only lead to mere shifts in the one-particle electronic dispersions and they are neglected from now in our study. Here, we assume that a *c* - *f* electron bounding state is equivalent to an exciton state.

Using Hartree-Fock approximation, we introduce the fluctuation operator $\delta A = A - \langle A \rangle$ for an arbitrary operator *A*, and write the Coulomb interaction operator in Eq. (4) as

$$\begin{aligned} c_{\mathbf{k}+\mathbf{q}}^\dagger c_{\mathbf{k}'} f_{\mathbf{k}'-\mathbf{q}}^\dagger f_{\mathbf{k}} = & \left[\langle f_{\mathbf{k}}^\dagger f_{\mathbf{k}}\rangle c_{\mathbf{k}'}^\dagger c_{\mathbf{k}'} + \langle c_{\mathbf{k}'}^\dagger c_{\mathbf{k}'}\rangle f_{\mathbf{k}}^\dagger f_{\mathbf{k}}\right] \\ & + \left[\langle c_{\mathbf{k}+\mathbf{q}}^\dagger f_{\mathbf{k}}\rangle f_{\mathbf{k}'-\mathbf{q}}^\dagger c_{\mathbf{k}'} + \langle f_{\mathbf{k}'-\mathbf{q}}^\dagger c_{\mathbf{k}'}\rangle c_{\mathbf{k}+\mathbf{q}}^\dagger f_{\mathbf{k}}\right] \end{aligned} \tag{5}$$

$$+\left[\langle c^{\dagger}_{\mathbf{k+q}} f_{\mathbf{k}}\rangle\langle f^{\dagger}_{\mathbf{k'-q}} c_{\mathbf{k'}}\rangle - \langle c^{\dagger}_{\mathbf{k+q}} c_{\mathbf{k'}}\rangle\langle f^{\dagger}_{\mathbf{k'-q}} f_{\mathbf{k}}\rangle\right]$$

Here, we only focus on the formation and condensation of excitons with momentum **q**. Therefore, constants here have been neglected in the approximation. In this case, the Hamiltonian in Eq. (1) reduces to the so-called Hartree-Fock Hamiltonian, which can be read

$$\mathcal{H}_{HF} = \sum_{\mathbf{k}} \bar{\varepsilon}^{c}_{\mathbf{k}} c^{\dagger}_{\mathbf{k}} c_{\mathbf{k}} + \sum_{\mathbf{k}} \bar{\varepsilon}^{f}_{\mathbf{k}} f^{\dagger}_{\mathbf{k}} f_{\mathbf{k}} + \Lambda \sum_{\mathbf{k}} \left(c^{\dagger}_{\mathbf{k+q}} f_{\mathbf{k}} + f^{\dagger}_{\mathbf{k}} c_{\mathbf{k+q}} \right) \tag{6}$$

here, the electronic excitation energies now have acquired Hartree shifts

$$\bar{\varepsilon}^{c(f)}_{\mathbf{k}} = \varepsilon^{c(f)}_{\mathbf{k}} + U n^{f(c)} \tag{7}$$

with $n^{f} = \frac{1}{N}\sum_{\mathbf{k}}\langle f^{\dagger}_{\mathbf{k}} f_{\mathbf{k}}\rangle$; $n^{c} = \frac{1}{N}\sum_{\mathbf{k}}\langle c^{\dagger}_{\mathbf{k}} c_{\mathbf{k}}\rangle$ are the densities of *f*- and *c*- electrons, respectively, where

$$\begin{aligned} \langle c^{\dagger}_{\mathbf{k}} c_{\mathbf{k}}\rangle &= \frac{1}{1+e^{\beta\bar{\varepsilon}^{c}_{\mathbf{k}}}} = n_F(\bar{\varepsilon}^{c}_{\mathbf{k}}) \\ \langle f^{\dagger}_{\mathbf{k}} f_{\mathbf{k}}\rangle &= \frac{1}{1+e^{\beta\bar{\varepsilon}^{f}_{\mathbf{k}}}} = n_F(\bar{\varepsilon}^{f}_{\mathbf{k}}) \end{aligned} \tag{8}$$

Here, $n_F(\in)$ is the Fermi-Dirac distribution function $n_F(\in) = \frac{1}{1+e^{\beta\in}}$ with $\beta = 1/T$ being the inverse of the temperature.

In effective Hamiltonian (6), Λ is an additional field, reads

$$\Lambda = -\frac{U}{N}\sum_{\mathbf{k}} \langle c^{\dagger}_{\mathbf{k+q}} f_{\mathbf{k}}\rangle \tag{9}$$

acts as an order parameter of the EI state. In previous letters, we addressed the EI phase diagrams and also the BCS-BEC crossover in the exciton systems via investigating the properties of the EI order parameter [17-19]. In this paper, we analyze the excitonic susceptibility creating an electron-hole excitation with momentum **q** in the system. The excitonic susceptibility function in momentum space is defined

$$\chi(\mathbf{q},\omega) = -\frac{1}{N}\sum_{\mathbf{k},\mathbf{k'}} \langle\langle f^{+}_{\mathbf{k}} c_{\mathbf{k+q}};\ c^{+}_{\mathbf{k'+q}} f_{\mathbf{k'}}\rangle\rangle_{(\omega)} \tag{10}$$

Using Hamiltonian (1) and writing the equation of motion for two-particle Green's function, we get

$$\begin{aligned} \omega\,\langle\langle f^{+}_{\mathbf{k}} c_{\mathbf{k+q}};\ c^{+}_{\mathbf{k'+q}} f_{\mathbf{k'}}\rangle\rangle_{(\omega)} &= \langle n^{f}_{\mathbf{k}}\rangle - \langle n^{c}_{\mathbf{k+q}}\rangle \\ &+\left(\varepsilon^{c}_{\mathbf{k+q}} - \varepsilon^{f}_{\mathbf{k}}\right)\langle\langle f^{+}_{\mathbf{k}} c_{\mathbf{k+q}};\ c^{+}_{\mathbf{k'+q}} f_{\mathbf{k'}}\rangle\rangle_{(\omega)} \\ -\frac{U}{N}\sum_{\mathbf{k_1 q_1}} \langle\langle \left(f^{+}_{\mathbf{k}} c_{\mathbf{k_1}} f^{+}_{\mathbf{k_1-q_1}} f_{\mathbf{k+q-q_1}} - c^{+}_{\mathbf{k+q_1}} c_{\mathbf{k_1}} f^{+}_{\mathbf{k_1-q_1}} c_{\mathbf{k+q}}\right);\ c^{+}_{\mathbf{k'+q}} f_{\mathbf{k'}}\rangle\rangle_{(\omega)} \end{aligned} \tag{11}$$

According to the principles of Hartree-Fock approximation, the excess operators in the higher order Green's functions are replaced by averages:

$$\sum_{\mathbf{k_1 q_1}} \langle\langle f^{+}_{\mathbf{k}} c_{\mathbf{k_1}} f^{+}_{\mathbf{k_1-q_1}} f_{\mathbf{k+q-q_1}};\ c^{+}_{\mathbf{k'+q}} f_{\mathbf{k'}}\rangle\rangle_{(\omega)}$$

$$= \sum_{\mathbf{q_1}} \langle n^{f}_{\mathbf{k+q-q_1}}\rangle\,\langle\langle f^{+}_{\mathbf{k}} c_{\mathbf{k+q}};\ c^{+}_{\mathbf{k'+q}} f_{\mathbf{k'}}\rangle\rangle_{(\omega)} \tag{12}$$

$$- \sum_{\mathbf{k_2}} \langle n^{f}_{\mathbf{k}}\rangle\,\langle\langle f^{+}_{\mathbf{k_2}} c_{\mathbf{k_2+q}};\ c^{+}_{\mathbf{k'+q}} f_{\mathbf{k'}}\rangle\rangle_{(\omega)}$$

$$\sum_{\mathbf{k_1 q_1}} \langle\langle c^{+}_{\mathbf{k+q_1}} c_{\mathbf{k_1}} f^{+}_{\mathbf{k_1-q_1}} c_{\mathbf{k+q}};\ c^{+}_{\mathbf{k'+q}} f_{\mathbf{k'}}\rangle\rangle_{(\omega)} \tag{13}$$

$$= \sum_{\mathbf{q_1}} \langle n^c_{\mathbf{k+q_1}} \rangle \langle\langle f^+_{\mathbf{k}} c_{\mathbf{k+q}};\ c^+_{\mathbf{k'+q}} f_{\mathbf{k'}} \rangle\rangle_{(\omega)}$$
$$- \sum_{\mathbf{k_2}} \langle n^c_{\mathbf{k+q}} \rangle \langle\langle f^+_{\mathbf{k_2}} c_{\mathbf{k_2+q}};\ c^+_{\mathbf{k'+q}} f_{\mathbf{k'}} \rangle\rangle_{(\omega)}$$

Replacing Eqs.(12) and (13) into Eq.(11), we obtain

$$\left(\omega - \omega^{cf}_{\mathbf{k}}(\mathbf{q})\right) \langle\langle f^+_{\mathbf{k}} c_{\mathbf{k+q}};\ c^+_{\mathbf{k'+q}} f_{\mathbf{k'}} \rangle\rangle_{(\omega)}$$
$$= \left(\langle n^f_{\mathbf{k}} \rangle - \langle n^c_{\mathbf{k+q}} \rangle\right) - \frac{U}{N}\left(\langle n^f_{\mathbf{k}} \rangle - \langle n^c_{\mathbf{k+q}} \rangle\right) \sum_{\mathbf{k_2}} \langle\langle f^+_{\mathbf{k_2}} c_{\mathbf{k_2+q}};\ c^+_{\mathbf{k'+q}} f_{\mathbf{k'}} \rangle\rangle_{(\omega)} \quad (14)$$

with $\omega^{cf}_{\mathbf{k}}(\mathbf{q}) = \bar{\varepsilon}^c_{\mathbf{k+q}} - \bar{\varepsilon}^f_{\mathbf{k}}$

Finally, we sum over **k** Eq. (14) and rename summation indices, the excitonic susceptibility function in Eq. (10) can be written

$$\chi(\mathbf{q}, \omega) = \frac{\chi^0(\mathbf{q}, \omega)}{1 + U\chi^0(\mathbf{q}, \omega)} \quad (15)$$

with

$$\chi^0(\mathbf{q}, \omega) = \frac{1}{N} \sum_{\mathbf{k}} \frac{\langle n^f_{\mathbf{k}} \rangle - \langle n^c_{\mathbf{k+q}} \rangle}{\omega - \omega^{cf}_{\mathbf{k}}(\mathbf{q})} \quad (16)$$

here $\langle n^f_{\mathbf{k}} \rangle = \langle f^\dagger_{\mathbf{k}} f_{\mathbf{k}} \rangle$ and $\langle n^c_{\mathbf{k}} \rangle = \langle c^\dagger_{\mathbf{k}} c_{\mathbf{k}} \rangle$ have been defined in Eq. (8).

In order to determine the EI phase, we compute the static excitonic susceptibility $\chi(\mathbf{q}, \omega)$ with $\omega = 0$. And in this work, we consider the direct bandgap situation so the order vector of the EI phase as $\mathbf{q} = 0$. Therefore, we focus on the condition for the divergence of the static excitonic susceptibility $\chi_0 = \chi(\mathbf{0}, 0)$ with respect to the temperature and the Coulomb interaction potential.

3. Numerical results and Discussions

To analyze the phase structure of the EI state, in this section, we present numerical results investigating the forming of the EI state in the system caused by the Coulomb interaction and the temperature. The value of excitonic susceptibility represents the exciton fluctuations in the system, in this work, therefore, the formation of the EI phase is indicated by the divergence of the static excitonic susceptibility χ_0. In doing so, the Eqs. (7), (8), (15) and (16) are solved self-consistently for a system containing $N = 500 \times 500$ lattice sites. The solution of the whole self-consistent calculation is assumed to be achieved if all quantities are determined with a relative error less than 10^{-12}. In our numerical calculation, the results are evaluated in the natural unit system for $\hbar = c = k_B = 1$ and without loss of generality all energies are given in units of the c electron transfer amplitude t^c, i.e., t^c =1. In this work, we choose $\varepsilon^c = 0$ and $t^f = 0.4 < t^c$ to fit the electron system state in rare-earth chalcogenide $TmSe_{0.45}Te_{0.55}$.

To discuss the impact of the temperature and the Coulomb interaction on the EI phase structure in the system, firstly, we show in Fig. 1 the dependence of the static excitonic susceptibility χ_0 on the Coulomb interaction U for various values of the temperature T at $\varepsilon^f = -1.5$. We see that the static excitonic susceptibility function only diverges or the EI phase only stabilizes at low temperature. At high temperature such as T = 0.5, the bound state of the electron–hole pairs is suppressed by the thermal fluctuations indicated by finite values of the static excitonic susceptibility for all values of U. In other words, at low temperature we always find the divergence of the static excitonic susceptibility at two critical values of the Coulomb interaction U_{c1} and U_{c2}. This means that the EI state only occurs in a confined between two critical values of the Coulomb interaction. Indeed, for $U < U_{c1}$ the weak Coulomb can neither form excitonic bound states nor establish the electron-hole coherence, the system settles in the SM state. Increasing U, the EI phase stabilizes above a critical Coulomb interaction U_{c1}. Similar to some recent studies [18-22], we also yield the upper critical value of the Coulomb interaction U_{c2}, such that the EI phase is confined in between U_{c1} and U_{c2}. As the temperature increases, U_{c1} increases while U_{c2}

decreases, so the window of the EI phase is narrowed. When $U > U_{c2}$, the Hartree shift leads to an electron-hole band splitting, that prevents *c-f* electron coherence and the system will be stable in the SC state.

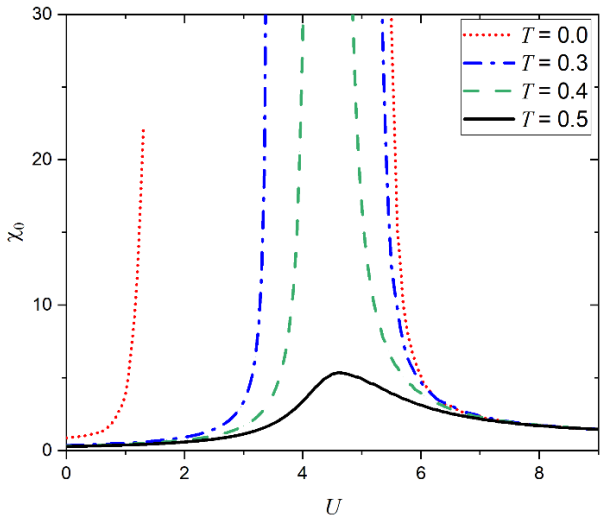

Fig. 1. The static excitonic susceptibility χ_0 as functions of the Coulomb interaction U for several values of temperature T.

Next, we discuss in detail the influence of the temperature on the EI state by investigating the dependence of the static exciton susceptibility function χ_0 on the temperature T for some values of the Coulomb interaction U at $\varepsilon^f = -1.5$ in Fig. 2. In the entire range of Coulomb interactions, we find that at a given Coulomb interaction, the static exciton susceptibility function increases as decreasing temperature. In particular, in low temperature region, the static exciton susceptibility increases strongly and diverges at a critical temperature T_{EI}. This is called the EI phase transition temperature. As $T > T_{EI}$ all excitonic bound states are deformed and the system is in the normal electron–hole liquid state. When $T < T_{EI}$, the system stabilizes in the EI state. Comparing the two panels in Fig. 2 (a and b), we once again affirm that the EI state is only occurred in between two critical values of the Coulomb interaction, a lower critical value U_{c1} and an upper critical value U_{c2}. The diagram also shows that if $U < 3.5$, the EI state exists at low temperature and the critical temperature T_{EI} increases as increasing U (see Fig. 2a), whereas T_{EI} decreases if enlarging from $U = 4.5$ (see Fig. 2b). In particular, if $U < 1.0$ or $U > 5.5$, the value of the static excitonic susceptibility function is so small and remains finite for all T.

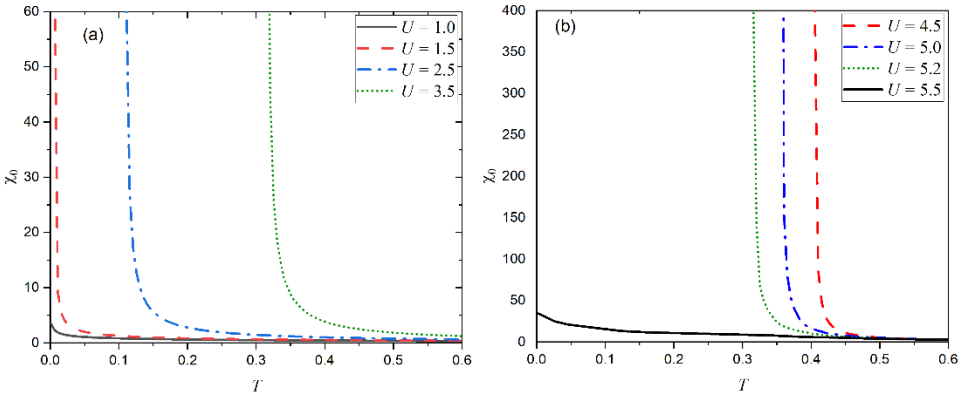

Fig. 2. The static excitonic susceptibility χ_0 as functions of the temperature T for several values of the Coulomb interaction U.

In order to confirm the existence of the EI state depending on the external pressure, we now present in Fig. 3 the static excitonic susceptibility χ_0 as functions of the temperature T for different values of *f*-electron on-site energy ε^f at the Coulomb interaction $U = 3.5$. Obviously, at a given ε^f, the formation of the EI phase is indicated by the divergence of χ_0 at the critical temperature T_{EI}. The diagram again shows

that the EI phase is only established at sufficiently low temperature. Increasing temperature, the large thermal energy destroys a part of the *c* - *f* electron bounding state leading to the EI state is weakened, which is illustrated by a decrease of the χ_0. As the temperature is larger than the critical temperature T_{EI}, the large thermal fluctuation breaks all the electron–hole couplings and the system settles in the electron–hole plasma liquid, and χ_0 thus becomes insignificant. Fig. 3 also shows that the critical temperature T_{EI} increases when increasing ε^f. Indeed, as ε^f is increased, the overlap between the *f*-bands and *c*-bands increases, then some *f* electrons can be transferred into *c*-band electrons and exciton bound states may be formed if the Coulomb interaction is sufficiently strong, therefore T_{EI} increases. In fact, the overlap between the energy bands represents the effect of the external pressure on the system. Therefore, increasing ε^f is corresponding to an increase of the external pressure. Our result about the influence of the temperature and the external pressure on the EI state fits quite well with the experimental observation in rare-earth chalcogenide $TmSe_{0.45}Te_{0.55}$ of P. Wachter [23]. At sufficiently large pressure, 4*f*- and 5*d*-bands overlap, then electrons from the *f*-band, which have been thermally excited into the 5*d* conduction band so 4*f*-holes couple to 5*d*-electrons to form excitons and then they can drop into the EI state if the temperature is sufficiently low.

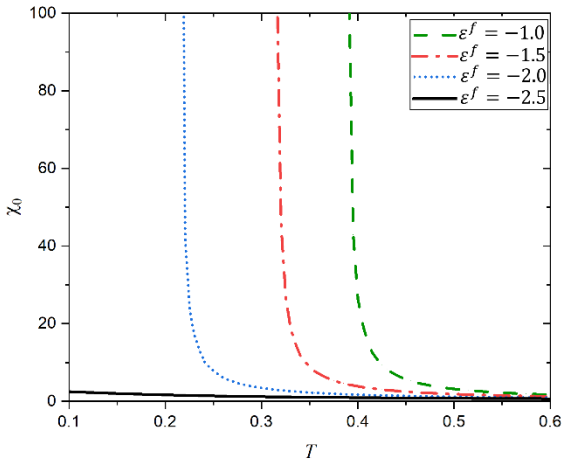

Fig. 3. The static excitonic susceptibility χ_0 as functions of the temperature *T* for different values of the on-site energy.

4. Conclusions

In this paper, we have adapted the unrestricted Hartree-Fock approximation to the 2D extended Falicov-Kimball model to investigate the EI state in rare-earth chalcogenides via analyzing the static excitonic susceptibility. As functions of model parameters, the phase diagrams of the EI state have been constructed. By analyzing the static excitonic susceptibility, we have found that when decreasing temperature, the exciton fluctuations strongly increase, especially near the temperature of the phase transition. As the temperature is low enough, the static excitonic susceptibility diverges which represents the EI phase transition. The critical temperature of the EI phase transition T_{EI} increases as increasing the Coulomb interaction *U* in the weak interaction regime. In contrast, T_{EI} decreases as increasing *U* in the strong Coulomb interaction regime. Our numerical results also have shown that at a given low temperature, the EI phase is found in between two critical values of the Coulomb interaction. When increasing temperature, the EI phase window is narrowed. In particular, the influence of the external pressure on forming of the EI state in the system also has been addressed. The phase diagram indicates that the EI state is formed only if the external pressure is sufficiently large. Considering more meticulously kinetic nature of the EI state in these materials would be a worthwhile goal of our studies in the future.

5. Acknowledgements

This research is funded by the Hanoi University of Mining and Geology, Vietnam, code T21-07.

The paper was presented during the 6th VIET - POL International Conference on Scientific-Research Cooperation between Vietnam and Poland, 10-14.11.2021, HUMG, Hanoi, Vietnam.

6. References

1. Mott, N.F., 1961. The transition to the metallic state. Philosophical Magazine, 6(62): 287-309, https://doi.org/10.1080/14786436108243318.
2. Knox, R., Theory of excitons, in Solid State Physics, edited by Seitz F. and Turnbull D., Academic Press, New York, 1963.
3. Kohn, W., Metals and insulator in Many Body Physics, edited by DeWitt C. & Balian R., Gordon & Breach, New York, 1968.
4. Moskalenko, S.A., Snoke, D.W., 2000. Bose-Einstein Condensation of Excitons and Biexcitons. Cambridge University Press, https://doi.org/10.1017/CBO9780511721687.
5. Neuenschwander, J., & Wachter, P., 1990. Pressure-driven semiconductor-metal transition in intermediate-valence $TmSe_{1-x}Te_x$ and the concept of an excitonic insulator. Physical Review B, 41(18), 12693, https://doi.org/10.1103/PhysRevB.41.12693.
6. Wachter, P., Bucher, B., & Malar, J., 2004. Possibility of a superfluid phase in a Bose condensed excitonic state. Physical Review B, 69(9): 094502, https://doi.org/10.1103/PhysRevB.69.094502.
7. Bucher, B., Park, T., Thompson, J.D., & Wachter, P., 2008. Thermodynamical Signatures of an Excitonic Insulator, Eprint arXiv:0802.3354.
8. Kogar, A., Rak, M.S., Vig, S., Husain, A.A., Flicker, F., Joe, Y.I., Venema, L., MacDougall, G.J., Chiang, T.C., Fradkin, E., et al., 2017. Signatures of exciton condensation in a transition metal dichalcogenide. Science, 358(6368): 1314 – 1317, https://doi.org/10.1126/science.aam6432.
9. Larkin, T.I., Yaresko, A.N., Pröpper, D., Kikoin, K.A., Lu, Y.F., Takayama, T., Mathis, Y.-L., Rost, A.W., Takagi, H., Keimer, B., & Boris A.V., 2017. Giant exciton Fano resonance in quasi-one-dimensional Ta_2NiSe_5. Physical Review B, 95(19): 195144, https://doi.org/10.1103/ PhysRevB.95.195144.
10. Lu, Y.F., Kono, H., Larkin, T.I., Rost, A.W., Takayama, T., Boris, A.V., Keimer, B. & Takagi, H., 2017. Zero-gap semiconductor to excitonic insulator transition in Ta_2NiSe_5. Nature Communication, 8, 14408, https://doi.org/10.1038/ncomms14408.
11. Ihle, D., Pfafferott, M., Burovski, E., Bronold, F.X., and Fehske, H., 2008. Bound state formation and the nature of the excitonic insulator phase in the extended Falicov-Kimball model. Physical Review B, 78(19): 193103, https://doi.org/10.1103/PhysRevB.78.193103.
12. Zenker, B., Fehske, H., & Batista C.D., 2010. Competing chiral and multipolar electric phases in the extended Falicov-Kimball model. Physical Review B, 82(16): 165110, https://doi.org/10.1103 /PhysRevB.82.165110
13. Sugimoto, K., Satoshi, N., Tatsuya, K., & Yukinori, O., 2018. Strong Coupling Nature of the Excitonic Insulator State in Ta_2NiSe_5. Physical Review letter, 120(24): 247602, https://doi.org/10.1103/PhysRevLett.120.247602.
14. Lee, J., Kang, C.J., Man, J.E., Jun, S.K., Byung, M., & Han, W.Y., 2019. Strong interband interaction in the excitonic insulator phase of Ta_2NiSe_5. Physical Review B, 99(7): 075408, https://doi.org/10.1103/PhysRevB.99.075408.
15. Bronold, F.X., & Fehske, H., 2006. Possibility of an excitonic insulator at the semiconductor-semimetal transition. Physical Review B, 74(16): 165107, https://doi.org/10.1103 /PhysRevB.74.165107.
16. Thang, D.V., Thao, D.T.X., 2012. Study the effect of rare earths Sm over physical $Bi_{1-x}Sm_xFeO_3$ of materials. Journal of Mining and Earth Science, 37, 86-91.
17. Hai, D.T.H., Nha, N.H., Giang, N.T., & Nham, P.V., 2016. Temperature effects in excitonic condensation driven by the lattice distortion. Physica Status Solidi B, 253(6): 1210-1216, https://doi.org/10.1002/pssb.201552745.
18. Hai, D.T.H., Hoi, B.D., & Nham, P.V., 2017. Phonon effects in the excitonic condensation induced in the extended Falicov-Kimball model, Europhysics Letters, 119, 47003,

https://doi.org/10.1209/0295-5075/119/47003

19. Hai, D.T.H., Nha, N.H., & Nham, P.V., 2019. Thermal Fluctuations in the Phase Structure of the Excitonic Insulator Charge Density Wave State in the Extended Falicov-Kimball Model, Journal of Electronic Materials, 48, 2677, https://doi.org/10.1007/s11664-018-06904-x.
20. Phan, N.V., Becker, K.W., & Fehske, H., 2010. Spectral signatures of the BCS-BEC crossover in the excitonic insulator phase of the extended Falicov-Kimball model. Physical Review B, 81(20), 205117, https://doi.org/10.1103/PhysRevB.81.205117.
21. Zenker, B., Ihle, D., Bronold, F.X. & Fehske, H., 2010. Existence of excitonic insulator phase in the extended Falicov-Kimball model: SO(2)-invariant slave-boson approach. Physical Review B, 81(11): 115-122, https://doi.org/10.1103/PhysRevB.81.115122.
22. Phan, N.V., Fehske, H. & Becker, K.W., 2011. Excitonic resonances in the 2D extended Falicov-Kimball model. Euro Physics Letter, 959(1): 17006, https://doi.org/10.1209/0295-5075/95/17006.
23. Wachter, P., 2018. Exciton Condensation and Superfluidity in $TmSe_{0.45}Te_{0.55}$. Advances in Materials Physics and Chemistry, 8(3): 120-142, https://doi.org/10.4236/ampc.2018.83009.